Pishniak, D., Beznoshchenko, B. (2020) Improving the detailing of atmospheric processes modelling using the Polar WRF model: a case study of a heavy rainfall event at the Akademik Vernadsky station.
Ukrainian Antarctic Journal, 2, 26—41.
https://doi.org/10.33275/1727-7485.2.2020.650

D. Pishniak*, B. Beznoshchenko

State Institution National Antarctic Scientific Center, Ministry of Education and Science of Ukraine, Kyiv, 01601, Ukraine

*** Corresponding author:** den.meteo.is@gmail.com

Improving the detailing of atmospheric processes modelling using the Polar WRF model: a case study of a heavy rainfall event at the Akademik Vernadsky station

Abstract. The Antarctic Peninsula region is of growing interest due to the regional climate change features and related atmospheric circulation patterns. The regional mesoscale atmospheric model Polar Weather Research and Forecasting (WRF) v4.1.1 was used in this research to study a heavy precipitation event over the Ukrainian Antarctic Akademik Vernadsky station region (Antarctic Peninsula). The passage of the cyclone over the Antarctic Peninsula as a typical synoptic process as well as a case of the daily precipitation maximum amount of 2018 were chosen for investigation in this research. The estimation of the modelling quality and downscaling was done by comparing the obtained results with in-situ observation at the Akademik Vernadsky station and cross-domain tracking of average meteorological values and their deviation. The concept of the nested domains allowed to increase the horizontal resolution of the simulated atmosphere up to 1 km and to reproduce the wind regime of this region with high quality. Comparison with measured data showed a significant improvement in wind simulation with increasing of resolution, but worse representation of surface temperature and humidity. The Polar WRF made a general cooling of near surface temperature of 2 °C during the period of simulation and increased precipitation amount by 4.6–8.4 mm (12–21%) on average over the territory relative to the initial data from Global Data Assimilation System. This can be explained by the contribution of noise and imperfection of the model (including static input data of the terrain description). Based on the modelled results, the interaction of wind flow with the mountainous terrain of the Antarctic Peninsula creates a range of complex dynamic effects in the atmosphere. These effects cause local precipitation maxima both over the Peninsula and over the adjacent ocean. These are, respectively, bay-valley areas of increased precipitation and increased precipitation on the crests of shock waves from orographic obstacles. Under certain background wind conditions, the influence of the latter effect can reach the Akademik Vernadsky station and cause the formation of heavy precipitation here.

Keywords: Antarctic Peninsula, downscaling, mesoscale atmospheric processes, numerical weather modelling, precipitation amplification effects, statistical evaluation

1 Introduction

The meteorology of Antarctic Peninsula region not only differs from the harsh conditions of cold continental Antarctica. This is also a special region in the Southern Hemisphere with its own regional characteristics. The mountain ridge as a significant obstacle for westerlies as well as a latitudinal orientation of the Antarctic Peninsula create regional atmospheric circulation in this region. Against the background of high synoptic activity and the influence of oceanic water masses, regional spatial climatic conditions are observed here, which are also displayed in the long term weather monitoring data from the meteorological stations (King & Comiso, 2003).

According to Turner et al. (2016), the last decadal temperature changes reflect the extreme natural internal variability of the regional atmospheric circulation in the Antarctic Peninsula region, rather than are associated with the drivers of global temperature change. Such local effects should be in each synoptic event. However, the small number of meteorological observation points in the Antarctic Peninsula region and their spatial distribution make it difficult to study these local atmospheric circulation effects.

The rapid development of global and mesoscale atmospheric models in recent years and increase in the spatial resolution of the modelling currently allow to use more detailed numerical and dynamic schemes at higher spatial and temporal resolution. Nowadays a range of operational global models and reanalyses with different spatial resolution covers the Antarctica region, i.e.: the European Centre for Medium-Range Weather Forecasts Global reanalysis (16 km), UK Met Office Unified Model (25 km), The Global Forecast System (GFS) by the National Centers for Environmental Prediction (28 km), The Global Spectral Model by the Japan Meteorological Agency (20 km), National Center for Atmospheric Research reanalyses etc.

But all of these models have typical and well known disadvantages: a) resolution inadequate to describe mesoscale features in key areas; b) physics not necessarily tuned for high latitudes; c) insufficient representation of surface features and Antarctic topography; d) inadequate initial conditions, reflecting the sparse observational network in the high southern latitudes (Bromwich et al., 2003). Therefore common practice is to use regional models (sub-models) for clarification of atmospheric conditions, taken from global models and complemented by additional data in research areas (Lazzara et al., 2020).

A number of studies have used atmospheric modelling as a tool to investigate the region. A comparative climate study of recent of the near-surface temperature trends representation over the Antarctic Peninsula in several models was done by Bozkurt et al. (2020). The importance of high resolution and advantage of using Polar Weather Research and Forecasting (Polar WRF) model for climate studying were discussed there. The biggest project of regional modelling (MM5 model, then Polar version of WRF) in Antarctica is known as Antarctic Mesoscale Prediction System (AMPS) (Bromwich et al., 2003; Powers et al., 2012). In this project the model was run with several nested domains down to 1 km resolution and 3 km over all Antarctic Peninsula. Thanks to this, several case studies were done for Amundsen Sea region and only a few for the Antarctic Peninsula. Kirchgaessner et al. (2019) using AMPS results made an estimation of foehn events over the Antarctic Peninsula. WRF model showed good skills in capturing the occurrence, frequency and duration of foehn events but underestimated the temperature increase and the humidity decrease during the foehn. Good representation of the foehn effect in Polar WRF model was obtained by Zhang and Zhang (2018).

A comprehensive evaluation of the Polar WRF version 3 performance in the Antarctic was done by Bromwich (2013). In the work it was shown that sources of initial data play the most important role in modelling skills, and the Planetary Boundary Layer (PBL) scheme may have influence on near surface temperature biases. Listowski and Lachlan-Cope (2017) showed that the surface longwave radiative bias is significantly reduced over the Larsen C Ice Shelf when using the Morrison, Thompson, and Milbrandt radiation schemes and lead to better agreement with aircraft cloud measurements. Deb et al. (2016) in the evaluation work of the high resolution Polar WRF simulation with nested domains over Antarctica noticed that Mellor-Yamada-Janjic (MYJ) PBL scheme shows generally the best results in comparison to others. Gómez-Navarro et al. (2015) during his case study of storm wind over the Alps reached the conclusion that only a high resolution domain (2 km) can provide adequate wind performance in mountain regions.

Weather observations at the Akademik Vernadsky station demonstrate often small-scale features in meteorological data series. One of the available ways to study and describe such features is to apply regional atmospheric models. The Polar WRF model is a commonly used solution for such purposes. That is why a case with a typical cyclone passage over the Antarctic Peninsula as well as a case of the daily precipitation maximum amount of 2018 was chosen for the investigation.

2 Data and Methods

2.1 General synoptic review

According to the synoptic charts of the Bureau of Meteorology (Australia's national weather, climate and water agency), the cyclone with frontal systems approached the Antarctic Peninsula and passed over it during April 14–16, 2018 (Fig. 1). In the first half of the 14th, the passage of a warm front over the station region was observed. The front was weakly expressed, which can be seen on satellite images of cloudiness over the region (Fig. 2). Later, by 15th 00 UTC, a cold front approached the station. It caused high intense precipitation at the Akademik Vernadsky station with maximum 24 mm per 12 hours (the biggest 12-h value of 2018) in the period 00–12 UTC April 15th. At the same time the jet-stream reached its greatest stage at the north–east part of the cyclone and over Antarctic Peninsula. The elongated meridional cloud field is well identified on satellite images near the Antarctic Peninsula. At this time, the cyclone began to cross the mountains of the Antarctic Peninsula and regenerated in the Weddell Sea. Towards the middle of the 15th, the cold front passed over the station, and the high-pressure ridge zone in the back part of the cyclone spread to the station.

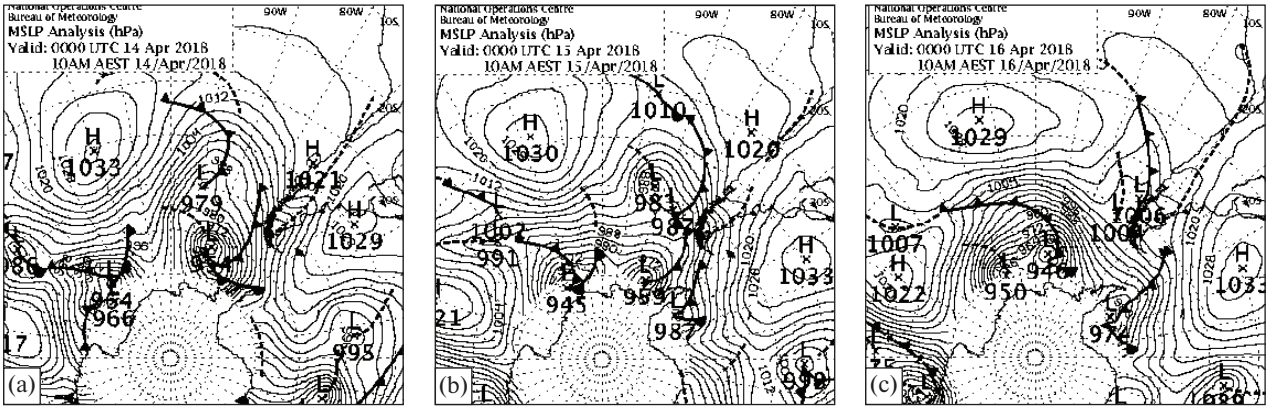

Figure 1. Synoptic situation in investigation period: (a) April 14, (b) April 15 and (c) April 16 2018 at 00:00 UTC. The cyclone crosses the ridge of the Antarctic Peninsula.

Source: Bureau of Meteorology, Australia's national weather, climate and water agency, http://www.bom.gov.au/

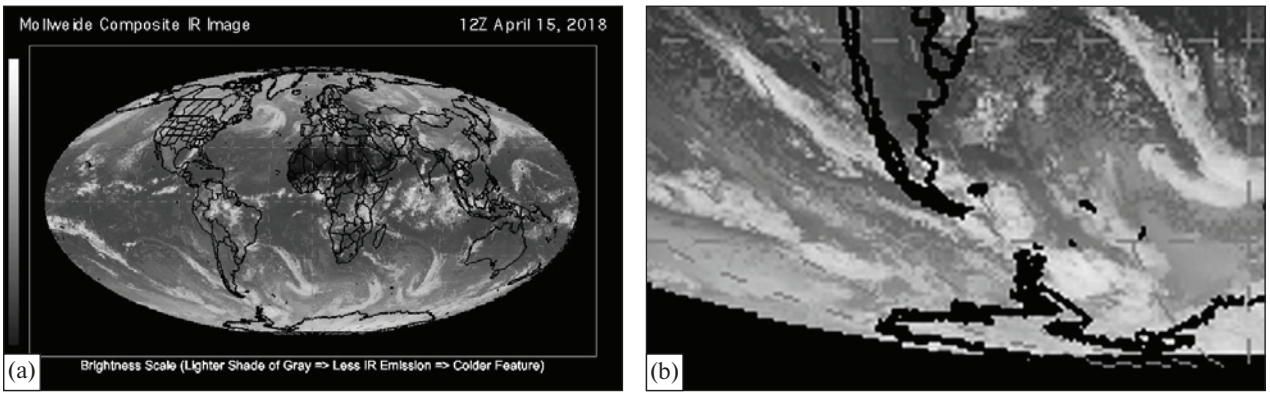

Figure 2. Infrared satellite image of clouds: (a) composite view, (b) zoomed fragment.

Source: California Regional Weather Server, sponsored by the Department of Earth & Climate Sciences, San Francisco State University. https://squall.sfsu.edu/crws/archive/composites_archive.html

2.2 Model configuration and research methods

The latest version of regional atmospheric model Polar Weather Research and Forecasting (Polar WRF) v4.1.1 was used for simulation of mesoscale atmospheric processes. This is a version of the WRF model that was modified and optimized for use in polar climates, developed by the Polar Meteorology Group of the Byrd Polar and Climate Research Center at The Ohio State University (Hines et al., 2011). Polar WRF provides options to more accurately represent conditions over the high latitudes and ice sheets. These adjustments to the thermal/radiative properties of ice and snow surfaces, include fractional sea ice representation and specification of sea ice albedo and snow depth on sea ice (Powers et al., 2017).

Initial and border conditions were taken from Global Data Assimilation System (GDAS, https://www.ncdc.noaa.gov/data-access/model-data/model-datasets/global-data-assimilation-system-gdas) primarily designed for launching NCEP Global Forecast System (GFS) operative model, USA. Time resolution of used GDAS datasets was 3 hours (analysis and 3h forecast from 00, 06, 12, 18 initial times). The model run was performed for 56.5 hours from 12 UTC 13 April 2018 till 20:30 UTC 15 April 2018 and included the selected rainfall event.

In order to analyze a chosen synoptic case, three domains were set in this study: 9-km resolution mother domain (domain D1) and two nested domains of 3-km (domain D2) and 1-km (domain D3) resolution respectively. The mother domain D1 consisted of 100 × 130 grid points and covered the whole Antarctic Peninsula region with a part of the Weddell Sea, Bellingshausen Sea and Pacific Ocean around the Antarctic Peninsula. Domain D2 had 175 × 175 grid points and included the north part of the Antarctic Peninsula. The lowest 1-km resolution domain D3 had 250 × 232 grid points and was centered at the region of Akademik Vernadsky station (Fig. 3). All domains were set at a grid ratio of 1 : 3. 48 vertical levels with a maximum height of 100 hPa were used for all domains.

Before choosing a projection, a map scale factor analysis was carried out for the selected region with

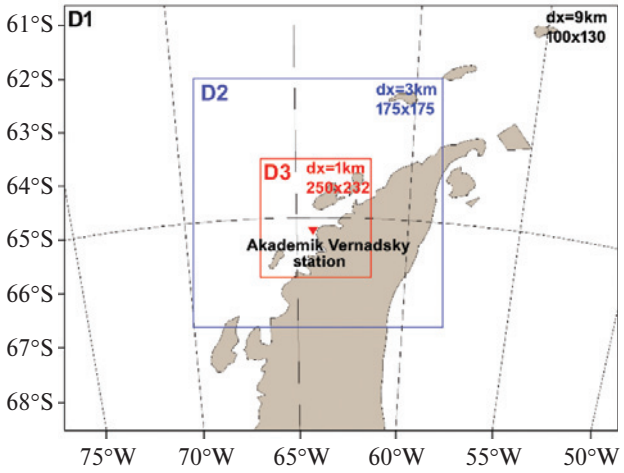

Figure 3. Polar WRF nested domains configuration

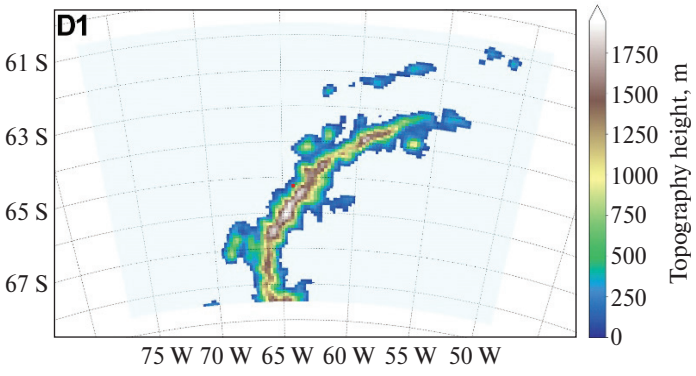

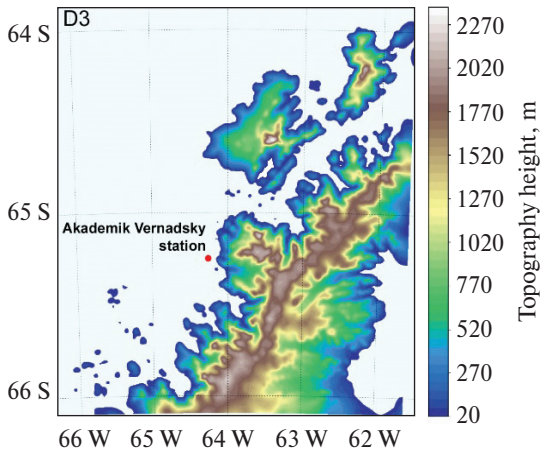

Figure 4. Polar WRF domains topography (domains D1 and D3) over Antarctic Peninsula region

the chosen domain configurations for three projections: Mercator, Lambert Conformal and Latitude-longitude. The Lambert conformal map projection showed the best results (Map Scale Factor for the biggest domain D1 is in range from 0.999 till 1.005) for the selected region over the Antarctic Peninsula. Therefore, all 3 domains were configured in the Lambert conformal map projection with the Standard longitude of 64.0 W and true latitudes 65.0 S and 60.0 S.

Because of the high domains resolution, in order to improve the quality of model calculations the standard relief dataset GTOPO30 with horizontal resolution of 1-km was replaced by the ASTER 1s topography dataset with horizontal resolution of 30 meters via QGIS module "GIS4WRF". Replaced topography height is shown on Fig. 4.

For the microphysics in the model input the New Thompson et al. (2008) scheme was set for the domain D1. The Morrison double-moment scheme and the WRF Single-Moment 3-class scheme were set for domain D2 and domain D3 respectively. The Noah land surface model (Noah LSM) was chosen as a surface layer physics option to calculate soil temperature and moisture. The Grell-Devenyi (GD) ensemble physical scheme as a Cumulus parameterization option was used only in domain D1 and domain D2, whereas convective rainfall was assumed to be explicitly resolved in domain D3. As options for describing the mechanisms of long-wave and short-wave radiation parameterization, Rapid Radiative Transfer Model and the Dudhia scheme were chosen respectively for all domains. The Mellor-Yamada-Janjic scheme which is a one-dimensional prognostic turbulent kinetic energy scheme with local vertical mixing was used for the PBL in the model input (Table 1). Full description of the WRF model principles, configurations and physical schemes are available in the Technical report by Skamarock et al. (2019).

To compare the simulation data with the measurements at the Akademik Vernadsky station, a nearest grid point to the station coordinates was taken for each domain using the Python programming language (Coordinates of selected points: the Akademik Vernadsky station: –65.2457, –64.2575; GDAS: –65.25, –64.25; Domain D1: –65.2460, –64.3440; Domain D2: –65.2460, –64.2793; Domain D3: –65.2459, –64.2581).

For statistical evaluation of the obtained results in the paragraph 3.1, such statistical coefficients were used: Correlation Coefficient, Root Mean Squared Error (RMSE), Mean absolute error (MAE) and Standard deviation of differences between modelling output data and observations.

For appropriate spatial comparison results of domains and models with different spatial resolution in the paragraph 3.1 we used averaging to the biggest cell size, which the GDAS model has. It means that

Table 1. WRF model configuration input options and physical parameterizations

Configuration option	Domain D1	Domain D2	Domain D3
Horizontal grids (grid points)	100 × 130	175 × 175	250 × 232
Horizontal resolution (km)	9	3	1
Vertical resolution (layers)	48	48	48
History interval (min)	30	15	10
Microphysics	New Thompson et al. scheme	Morrison double-moment scheme	WRF Single-Moment 3-class scheme
Longwave radiation	RRTM scheme		
Shortwave radiation	Dudhia scheme		
Planetary boundary layer	Mellor-Yamada-Janjic scheme		
Cumulus parameterization	Grell-Devenyi (GD) ensemble scheme		NONE
Land surface	Noah Land Surface Model		
Surface layer	Eta similarity scheme		

high resolution data from the WRF model were smoothed to 0.25 degree horizontal grid before making comparison. On the other hand the area of investigation was limited by the smallest domain WRF D3 (250 × 232 km), to make evaluation on the same territory through all the models and domains.

3 Results

3.1 Evaluation of the modelled and observed data and their comparison

Statistical analysis using selected standard criteria did not show unambiguous results. Although most results of modelling on coarsened grid were better compared to observations than modelling on a small grid (Table 2), especially for the temperature and humidity data. Only for wind speed the values criteria for the domain D3 are better than for domain D1 and domain D2. In fact, this is a typical effect of the contribution of noise from small-scale meteorological processes and turbulence on a small grid, together with an increase in the imperfection of atmospheric models on small scales. In this case, under the imperfection of the model, we also understand the poor representation of the terrain and other properties of the underlying surface that need some clarification.

Obviously, for adequate statistical comparison of the different spatial resolution results of the modelling, it is necessary to use special methods or approaches that are the subject for further research and discussion. That is why below we tried to make a comparison based on the physical interpretation of the processes.

In general, Fig. 5 shows that the modelled results on the domains D3 and D2 had much more small features than the results of the parent domain D1 and, especially, input GDAS data. The fluctuations of meteorological parameters in the observed data are most

Table 2. Statistical evaluation of the model results to in-situ observations at the Akademik Vernadsky station

Domain / Model	N	Correlation	RMSE	MAE	Standard deviation of errors
			Temperature		
GDAS	19	0.71	0.36	1.28	0.87
D1	114	0.79	0.86	1.25	0.81
D2	114	0.78	0.59	0.24	0.99
D3	340	0.46	2.15	1.41	1.63
			Humidity		
GDAS	19	0.85	2.14	7.13	5.76
D1	114	0.84	3.30	1.96	5.37
D2	114	0.83	3.71	3.05	5.65
D3	340	0.60	9.85	3.00	9.39
			Sea Level Pressure		
GDAS	19	0.97	0.43	1.45	1.12
D1	114	0.98	1.07	1.58	0.97
D2	114	0.98	1.09	1.56	1.04
D3	340	0.97	1.79	1.40	1.12
			Wind Speed		
GDAS	19	0.18	0.97	0.03	4.21
D1	114	0.42	5.75	8.75	4.72
D2	114	0.39	3.94	5.20	4.40
D3	340	0.50	4.59	1.90	4.19

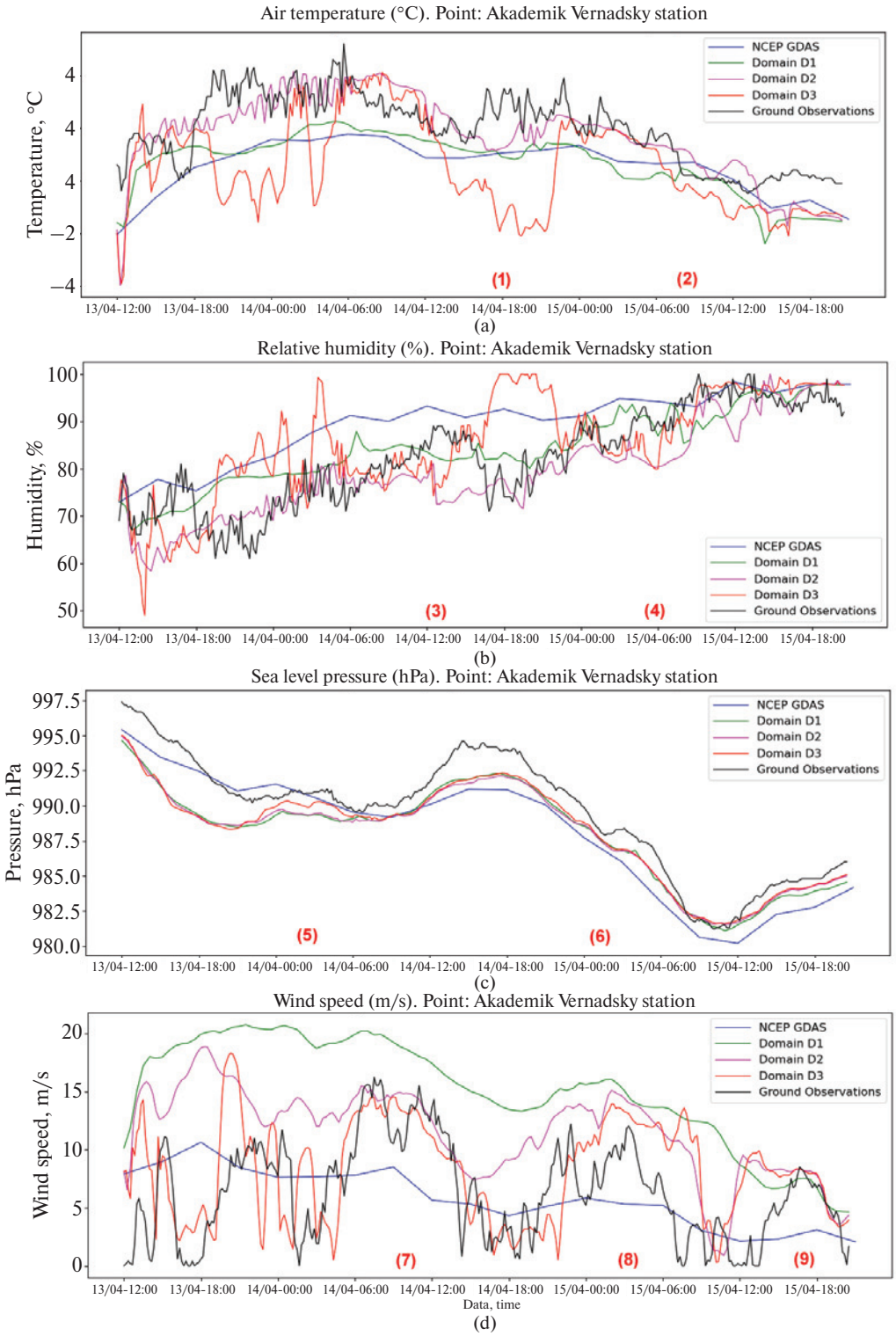

Figure 5. Meteorological time-series at the Akademik Vernadsky station and in the nearest models grid points: 2m air temperature (a), 2m relative humidity (b), sea level pressure (c) and wind speed (d)

similar to the results for the D3 domain, so we interpreted these curves with meteorological processes.

In the temperature graph (Fig. 5a) as same as in the Table 2, domain D2 showed the best results. A short-term decline separating two large waves of temperature rise on the temperature graph near position (1) was identified. This process can be seen for all domains, but in the model results it is slightly shifted and shortened in duration than the observation data reality. Position (2) corresponds to the moment of passage of the atmospheric front in the temperature field and here the result of modelling corresponds to the actual observations very well (the difference is within 20 min).

As can be seen on the relative humidity graph (Fig. 5b), the Polar WRF and GDAS both showed overestimated values over Akademik Vernadsky station, which logically corresponds to the general underestimation of the temperature at the model grid point. In the relative humidity trend of the domain D3 (red curve), there are two noticeable declines in (3), (4) against the background of steady increase in humidity values. Here, the humidity curve mirrors the corresponding temperature curve in the temperature graph above. This is a characteristic feature of the foehn effect. At the same time the black curve of the measured humidity also has a tendency to mirror the temperature on the graph above. Thus, the two heat waves traced on the graphs of the D3 modelling results and

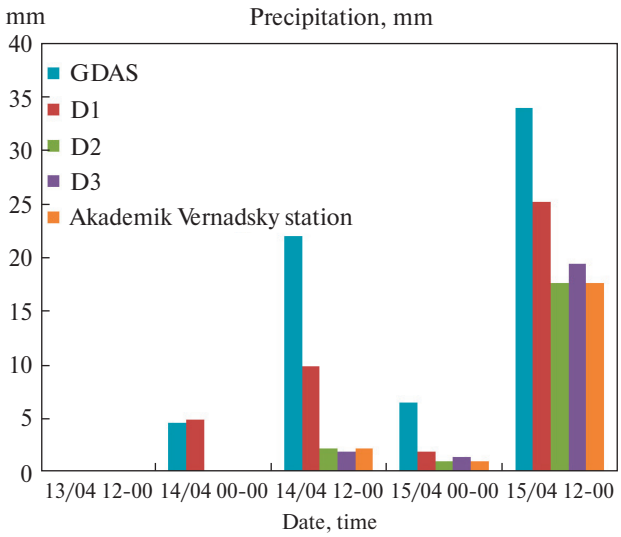

Figure 6. 12 hours sum (in-situ observation time) of precipitation at the Akademik Vernadsky station

actual observations (Fig. 5a) are the same foehn effect that is presented in the model with some delay.

Near (5), (6) on the sea level pressure graphs (Fig. 5c), the small features of the modelled pressure timeline of the D3 domain correspond to the ground observations quite well, which relate to the passage of certain mesoscale meteorological processes over the station. The graph of ground observations has smaller fluctuations than the 1 km resolution model can show. Obviously, this is the effect of quite powerful micro-

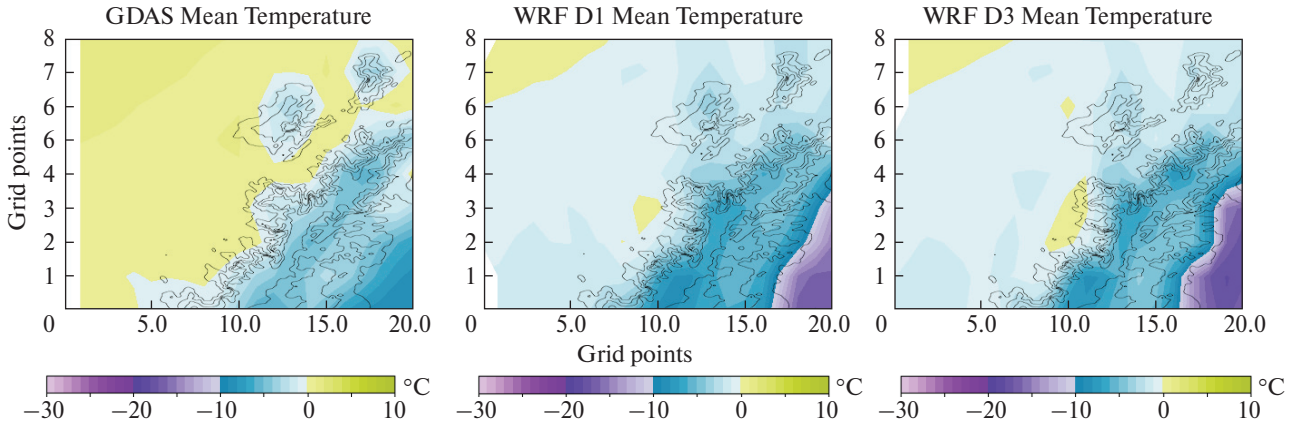

Figure 7. Mean temperature fields over the smallest domain area. High resolution data of Polar WRF model were coarsened to 0.25 degree horizontal grid, identically to initial GDAS dataset. Black lines outline land and mountains

processes of turbulence of sub-kilometer scale which exist in this area.

In the wind graph (Fig. 5d), two episodes of strong wind (7), (8) perfectly fitted the modelled data of the D3 domain and corresponded to the foehn effect observed on temperature and humidity graphs. The frontal increasing in wind speed (9) was also well reproduced by modelling in domains D3 and D2.

In case of precipitation data the initial GDAS model inadequately overestimated the amount of precipitation in the closest to the Akademik Vernadsky station grid point (Fig. 6). The first domain D1 data of the Polar WRF model occupied a transitional position, while the amount of precipitation in domains D2 and D3 already corresponds well with ground measurements.

Thus, despite the worse values of used statistical parameters, high-resolution modelling (D3 domain) showed the best reflection of mesoscale processes that influence the variation of meteorological parameters at the Akademik Vernadsky station.

3.2 Evaluation of the downscaling

General correspondence/deviation of the model simulation to the global analysis (GDAS) was examined on fields of temperature and precipitation over the area of domain D3. Biases of the domain D3 data to domain D1 are also presented below.

It should be noticed that the Polar WRF model decreased the near surface temperature over the domain areas including open ocean, mountains and especially over the Larsen Ice Shelf (Fig. 7, Table 3). Only several cells over the mountain had positive temperature biases (Fig. 8). Mean value of Polar WRF D1 temperature biases to GDAS values for the entire area and period was –2.07 °C (Table 4), which is similar to the results obtained by Bromwich (2013) for the current PBL scheme in summer time over Antarctica. On time plot ensemble not only changeable time dependencies in biases for some cells were noticed but also general trend to negative bias growing during modelling time (Fig. 8).

With further increase in resolution of the Polar WRF model, foothills and mountain slopes became warmer except the Larsen Ice Shelf, which similarly to the domain D1 became colder. Therefore the mean area value of temperature from domain D1 to domain D3 did not change (bias = +0.01 °C). This may be explained by the better description of orographic effects and precipitation formation regarding the increase in the domain resolution. In general, temperature biases between GDAS and the Polar WRF as same as between downscaling domains in the Polar WRF is bigger in cells over mountain slopes at both sides of the Antarctic Peninsula. They have explicit and variable time dependencies which mean strong relation to synoptic conditions over the region (Fig. 8).

The precipitation amount distribution over the studied domain was not well presented in the GDAS model in relation to the relief details. Some peaks in

Table 3. The mean values over research domain for all simulation period

Value	GDAS	Polar WRF D1	Polar WRF D2	Polar WRF D3
2m Temperature	–0.90 °C	–2.97 °C	–2.89 °C	–2.96 °C
Accumulated Precipitation	39.7 mm	44.2 mm	48.8 mm	48.6 mm

Table 4. Mean biases over research domain for all simulation period

Value	Polar WRF D1 vs GDAS	Polar WRF D2 vs Polar WRF D1	Polar WRF D3 vs Polar WRF D1
Bias of Temperature	–2.07 °C	+0.08 °C	+0.01 °C
Bias of Accumulated Precipitation	+4.6 mm (+12%)	+4.6 mm (+10%)	+4.4 mm (+10%)

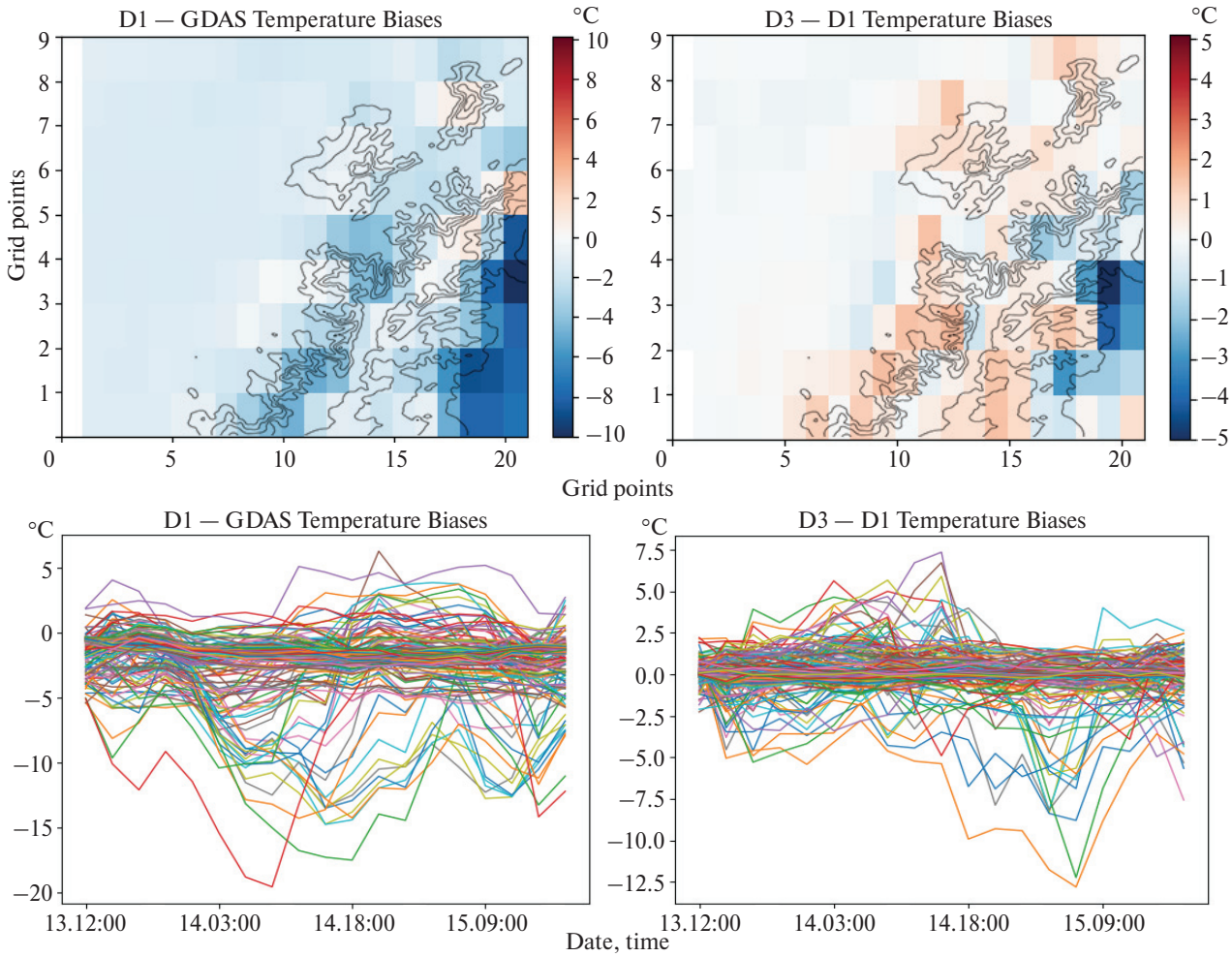

Figure 8. Spatial and time distribution of the near surface temperature biases for each point of the coarsened grid

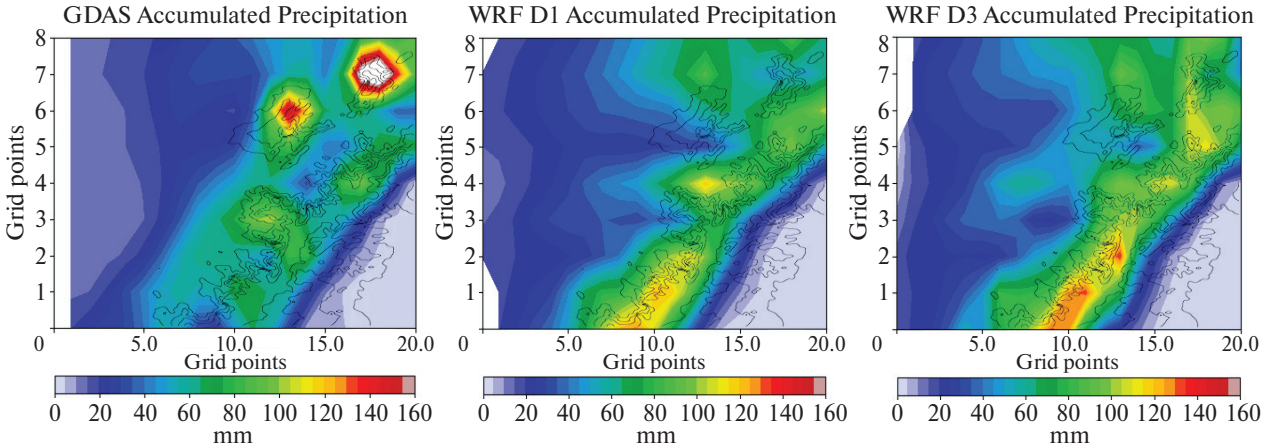

Figure 9. Accumulated precipitation over the smallest domain area. High resolution data of Polar WRF model were coarsened to the 0.25 degree horizontal grid, identically to the initial GDAS dataset. Black lines outline land and mountains

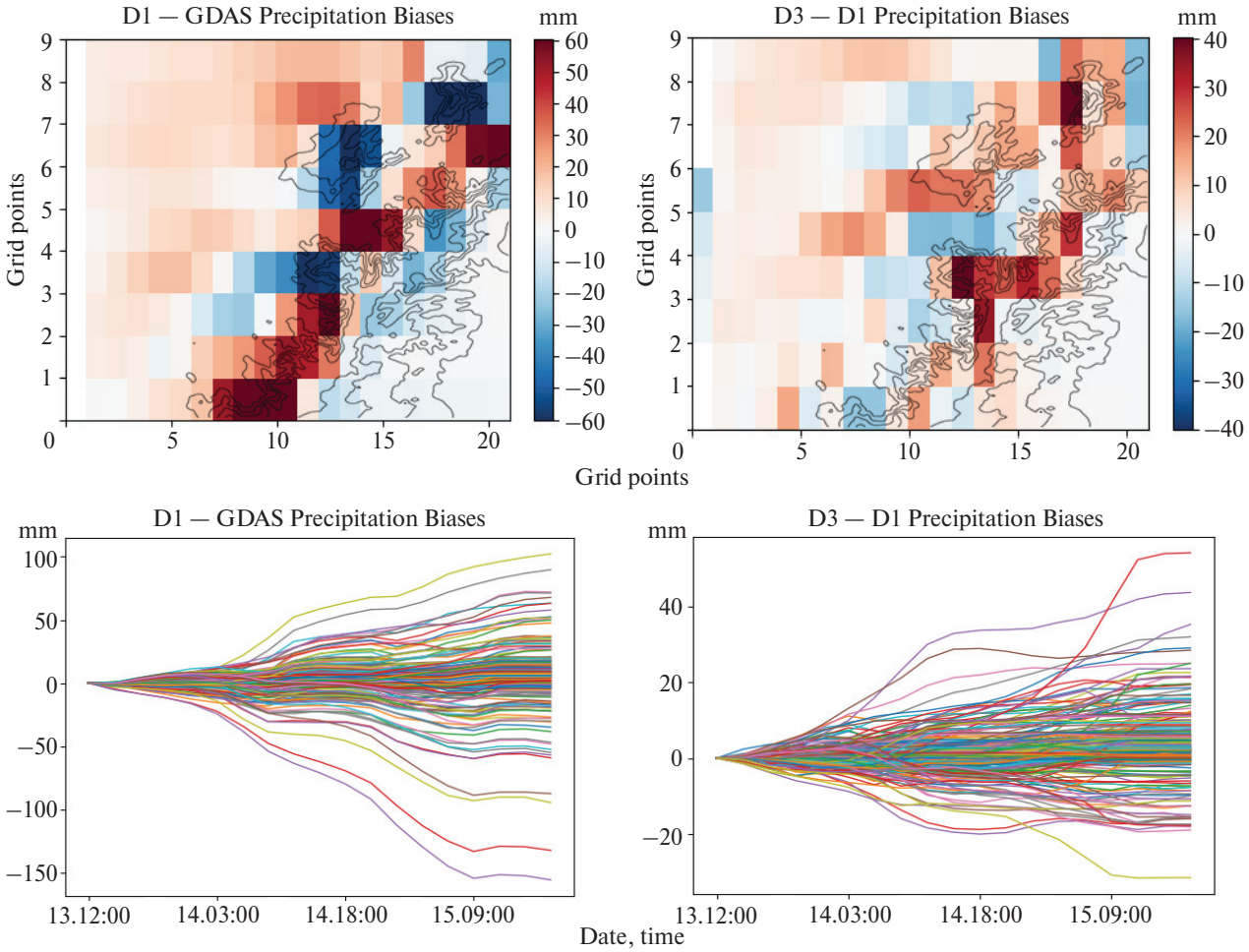

Figure 10. Spatial and time distribution of accumulated precipitation biases for each point of the coarsened grid

distribution look unreasonable (Fig. 9). Polar WRF model in domain D1 with resolution of 9 km showed much better correspondence of the distribution to the mountains. This produced huge irregular biases between models on the west coast of the Antarctic Peninsula (Fig. 10). But the WRF model also showed the higher precipitation over the open ocean, which should relate to the differences in models physics rather than influence of topography and resolution. In average, WRF model increased the precipitation amount by 4.6 mm (12%) over the studied domain in modelling period (Table 4).

Further downscaling from domain D1 to D3 demonstrated less significant redistribution of the precipitation amount. Its peaks slightly shifted to the mountain tops and had the best fit to the topography even after coarsening of resolution for the analysis. Thus downscaling in the WRF model increased precipitation over mountain ridges and decreased it near foothills of the Antarctic Peninsula west coast. In general downscaling increased precipitation amount by 4.4 mm (10%) over the domain D3, but this happened on transition to domain D2 and then preserved to domain D3 (Table 4).

The time dependent Polar WRF to GDAS biases ensemble demonstrated high stability of trends compared to the more variable WRF D3 to D1 trends (Fig. 10). Hence in the first case biases will weakly depend on the synoptic condition, while in the second it should have a stronger relation to the large-scale atmospheric situation.

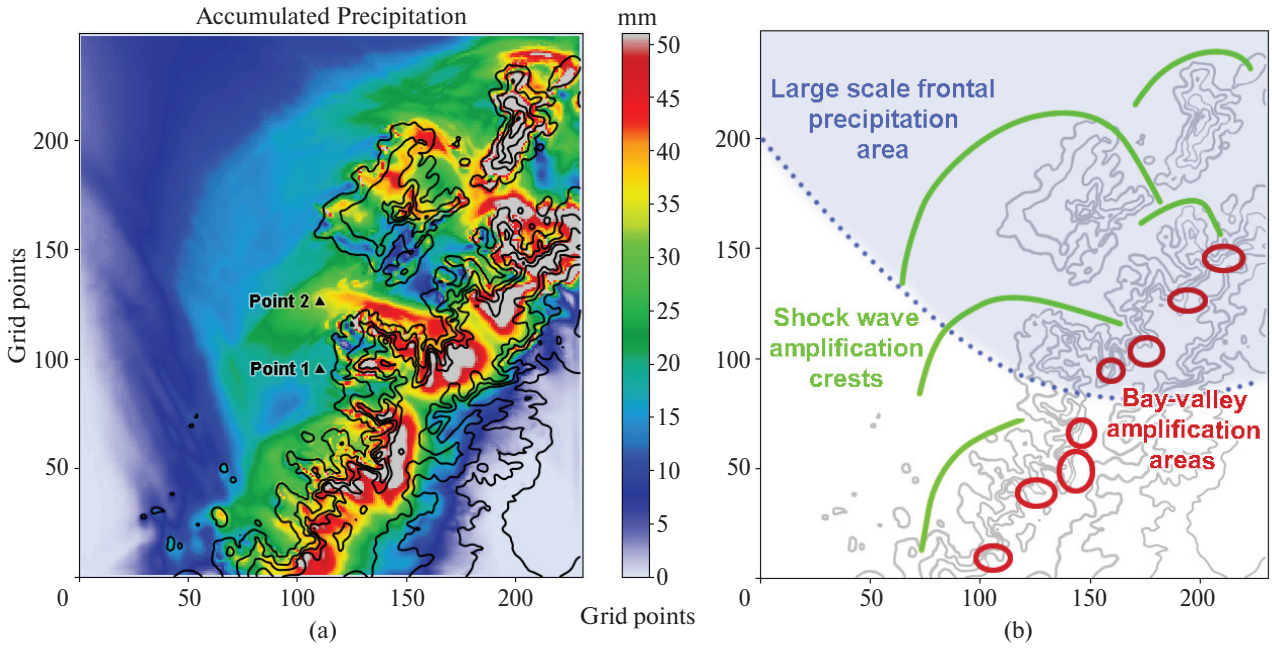

Figure 11. Model simulation of extreme precipitation event at 00–12 UTC 15 April 2018, accumulated precipitation in domain D3 (a) and schematic positions of mesoscale precipitation amplification effects (b). Black lines outline land and mountains, grid points correspond to distance in km for current domain

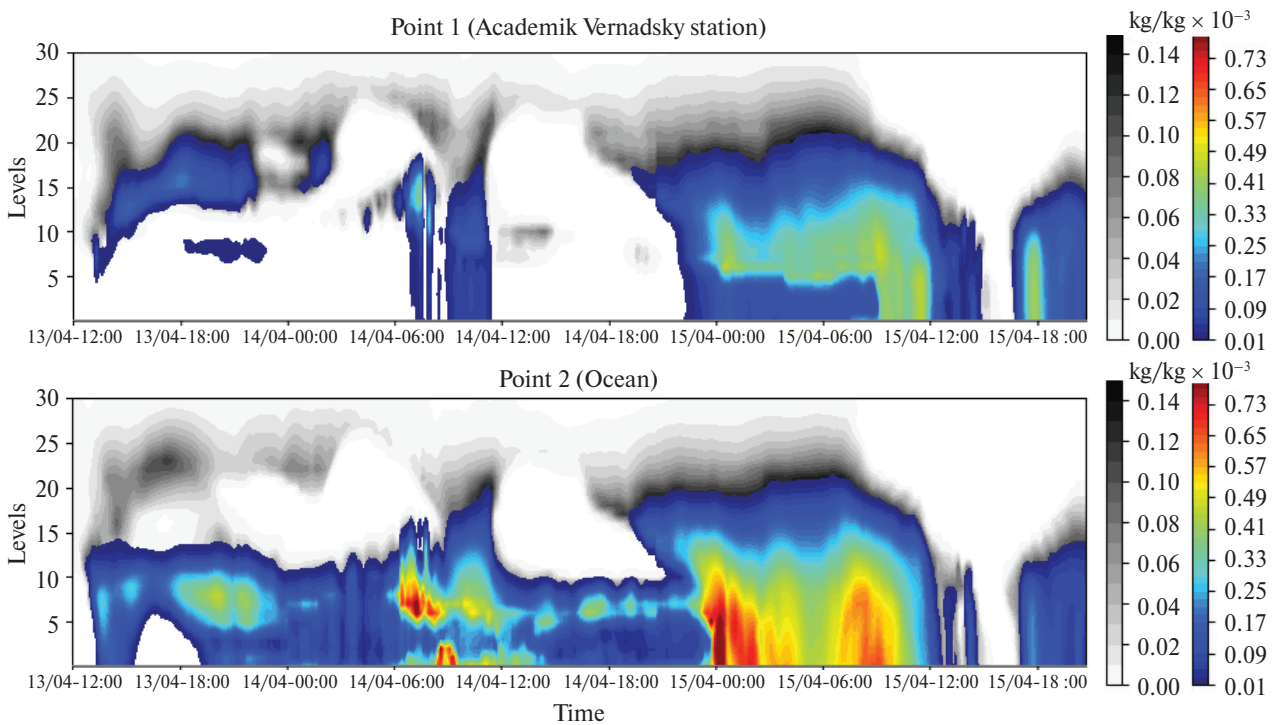

Figure 12. Time-height cross-section of Rain water (equivalent of precipitation intensity, colored) and Cloud water (grayscale) over the Akademik Vernadsky station (Point 1) and 30 km to the North, over ocean (Point 2, Fig. 11a). Vertical levels are irregular from 0 to 9 km height. Physical unit is a mass of water in a unit mass of air (kg/kg)

Only temperature and precipitation were chosen for this type of analysis, since wind speed and pressure values directly depend on topography height and need additional preparation to exclude this effect in such a mountainous region.

3.3 Detailed structure of the atmospheric processes

The modelling showed that the mesoscale distribution of precipitation in the region depends not only on the height of the terrain and the orientation of the slopes, but mainly on the mesoscale perturbations of the atmosphere formed by the configuration of mountains and extending 10–100 km from their generation. It can be identified as low level wind-induced precipitation amplification effects that are formed by strong winds in the lower layer of the troposphere and quickly disappear when wind decreases. In particular, it was noticed that along the ridge of the Antarctic Peninsula, the amount of precipitation varies twice (from 30 to 60 mm in 12 hours, Fig. 11a) with maxima located in front of the basins of sea bays. Apparently, it was caused by the typical funnel-shaped configuration of the bays, which redirects the oncoming northern air flow into a vertical, ascending stream at the end of the basin. The schematic positions of these mesoscale structures called *Bay-valley amplification areas*, in the studied case are presented on Fig. 11b.

Another dynamic effect that affects the distribution of precipitation is *Shock wave amplification crests* from significant orographic obstacles in the flow path. This effect extends on long distances over the open ocean in the form of bands encircling ledges of the peninsulas and islands. Under certain wind conditions, the Akademik Vernadsky station may be under influence of this effect. But as the current simulations showed, the axis of the maximum of nearest shock wave amplification effect is 20–40 km north of the station.

To study and compare how the vertical structure of precipitation at the Akademik Vernadsky station differs from the central line of the shock wave precipitation maximum, two time-height cross-sections of the parameters Rain Water and Cloud Water in the Polar WRF model were plotted (Fig. 12).

According to the model results, the origin of precipitation over the Akademik Vernadsky station occurred only in the upper and middle troposphere. During the period of intense precipitation (22:00 UTC on April 14 — 14:00 UTC on April 15), a significant increase in precipitation particles was observed in the lower troposphere, which explains a high intensity of the precipitation at this time. By 09:00 UTC it was in the form of rainfall with a melting zone at an altitude of 300 m, and then turned into snowfall (Fig. 12, Point 1).

At the same time, low clouds at altitudes of 500–1500 m constantly produced small precipitation in the crest of a shock wave 30 km northern from the station above the ocean surface (Fig. 12, Point 2). When the cloudiness of the main front approached in the upper and middle atmosphere, the intensity of precipitation increased significantly and twice exceeded their intensity at the Akademik Vernadsky station, according to simulation. Although at the Akademik Vernadsky station measured precipitation amount record of 2018 was registered. At this time in Point 2 precipitation fell only in the form of snowfall and the air temperature was constantly lower by 1–3 degrees.

4 Conclusion

Statistical comparison of the modelling results, obtained via the Polar WRF v4.1.1, and ground observations at the Ukrainian Antarctic Akademik Vernadsky station did not show a direct improvement of the modelling quality with increasing the resolution in the studied case. According to standard criteria and meteorological parameters, modelling on coarsened domains had an advantage compared to high-resolution domains, while for others criteria — vice versa. It was caused by the increase in influence of random noise in high-resolution simulations. More correct comparison of the quality of modelling on different nested domains requires the usage of specialized methods or approaches.

The most obvious leap in meteorological fields appeared during the transition between models GDAS and Polar WRF. It was caused not only by resolution and topography changes but also by the differences in physical description of the atmosphere. A smaller leap appeared after transition from domain D1 to domain

D2 of the Polar WRF, with resolution 9 km and 3 km respectively. But such a leap was almost absent in transition to domain D3 with the spatial resolution of 1 km. In fact, the Polar WRF made a general cooling of near surface temperature of 2 °C during the period of simulation and increased precipitation amount by 4.6–8.4 mm (12–21%) on average over the territory relative to the initial GDAS data. Also downscaling facilitates a better correspondence of meteorological fields to the topography features even after turning the spatial resolution to the initial 0.25 × 0.25 degrees (26 × 11 km).

Generally, the analysis showed that increasing the resolution of the domain led to a significant increase in the representation of wind and precipitation fields (i.e. improved the atmospheric dynamics representation). While the representations of radiation balance, turbulence and other physical components which are responsible for temperature and humidity in the model were less dependent on the spatial resolution.

Only high resolution domain D3 showed the key structure of mesoscale atmospheric processes which led to the formation of extreme precipitation and windstorm conditions. Thus the simple orographic lifting of air mass accompanied by more complex dynamic effects initialized by air flow-terrain interaction were identified in precipitation fields. It included Bay-valley amplification areas and Shock wave amplification crests which complemented the large scale frontal precipitation zone of the cyclone. In certain wind conditions the Shock wave amplification crests may reach Akademik Vernadsky station and increase precipitation intensity to extreme level.

The usage of high-resolution models creates new opportunities for studying mesoscale atmospheric processes and features of the microclimate in the Antarctic Peninsula region. However, a cross-scale comparison of the modelling quality and evaluating the quality of high-resolution modelling need focused attention in further studies. Complex dynamic effects of precipitation intensity in the Antarctic Peninsula region should be analyzed in extended and more purposeful further studies.

Author contributions. DP: main idea, editing meaning and content, post-processing of model output, writing the parts of the article: 1 Introduction, 3.1 Evaluation and comparison of the modelled and observation data, 3.2 Evaluation of the downscaling, 3.3 Detailed structure of the atmospheric processes, 4 Conclusion. BB: model adjustments and supporting the modelling process, post-processing of model output, writing the parts of the article: 1 Introduction, 2.1 General synoptic review, 2.2 Model configuration and research methods. 3.1 Evaluation and comparison of the modelled and observation data.

Conflict of Interest. The authors declare that they have no conflict of interest.

Acknowledgements. This work was supported by the State Institution National Antarctic Scientific Center, Ministry of Education and Science of Ukraine, according to State Special-Purpose Research Program in Antarctica for 2011–2020.

References

Bozkurt, D., Bromwich, D. H., Carrasco, J., Hines, K. M., Maureira, J. C., & Rondanelli, R. (2020). Recent near-surface temperature trends in the Antarctic Peninsula from observed, reanalysis and regional climate model data. *Advances in Atmospheric Sciences*, 37, 477—493. https://doi.org/10.1007/s00376-020-9183-x

Bromwich, D. H., Monaghan, A. J., Powers, J. G., Cassano, J. J., Wei, H-L., Kuo, Y-H., & Pellegrini, A. (2003). Antarctic Mesoscale Prediction System (AMPS): a case study from the 2000–01 field season. *Monthly Weather Review*, 131(2), 412–434. https://doi.org/10.1175/1520-0493(2003)131<0412:AMPSAA>2.0.CO;2

Bromwich, D. H., Otieno, F. O., Hines, K. M., Manning, K. W., & Shilo, E. (2013). Comprehensive evaluation of polar weather research and forecasting model performance in the Antarctic. *Journal Of Geophysical Research: Atmospheres*, 118(2), 274–292. https://doi.org/10.1029/2012JD018139

Deb, P., Orr, A., Hosking, J. S., Phillips, T., Turner, J., Bannister, D., Pope, J. O., & Colwell, S. (2016). An assessment of the Polar Weather Research and Forecasting (WRF) model representation of near-surface meteorological variables over West Antarctica. *Journal of Geophysical Research: Atmospheres*, 121(4), 1532–1548. https://doi.org/10.1002/2015JD024037

Gómez-Navarro, J. J., Raible, C. C., & Dierer, S. (2015). Sensitivity of the WRF model to PBL parametrisations and nesting techniques: evaluation of wind storms over complex terrain. *Geoscientific Model Development,* 8, 3349–3363. https://doi.org/10.5194/gmd-8-3349-2015

Hines, K. M., Bromwich, D. H., Bai, L.-S., Barlage, M., & Slater, A. G. (2011). Development and testing of Polar WRF.

Part III: Arctic Land. *The Journal of Climate*, 24(1), 26–48. https://doi.org/10.1175/2010JCLI3460.1

King, J. C., & Comiso, J. C. (2003). The spatial coherence of interannual temperature variations in the Antarctic Peninsula. *Geophysical Research Letters*, 30(2), Article 1040. https:// doi.org/10.1029/2002GL015580

Kirchgaessner, A., King, J., & Gadian, A. (2019). The representation of Föhn Events to the East of the Antarctic Peninsula in simulations by the Antarctic Mesoscale Prediction System. *Journal of Geophysical Research: Atmospheres*, 124(24), 13663–13679. https://doi.org/10.1029/2019JD030637

Lazzara, M. A., Orendorf, S. A., Norton, T. P., Powers, J. G., Bromvich, D. H., Carpentier, S., Cassano, J. J., Colwell, S. R., Cayette, A. M., & Werner, K. (2020). The 13th and 14th Workshops on Antarctic Meteorology and Climate. *Advances in Atmospheric Sciences*, 37, 423–430. https://doi.org/10.1007/s00376-019-9215-6

Listowski, C., & Lachlan-Cope, T. (2017). The microphysics of clouds over the Antarctic Peninsula — Part 2: modelling aspects within Polar WRF. *Atmospheric Chemistry and Physics*, 17, 10195–10221. https://doi.org/10.5194/acp-17-10195-2017

Powers, J. G., Manning, K. W., Bromwich, D. H., Cassano, J. J., & Cayette, A. M. (2012). A decade of Antarctic science support through AMPS. *Bulletin of the American Meteorological Society*, 93(11), 1699–1712. https://doi.org/10.1175/BAMS-D-11-00186.1

Powers, J. G., Klemp, J. B., Skamarock, W. C., Davis, C. A., Dudhia, J., Gill, D. O., Coen, J. L., Gochis, D. J., Ahmadov, R., Peckham, S. E., Grell, G. A., Michalakes, J., Trahan, S., Benjamin, S. G., Alexander, C. R., Dimego, G. J., Wang, W., Schwartz, C. S., Romine, G. S., ... & Duda, M. G. (2017). The Weather Research and Forecasting Model: Overview, system efforts, and future directions. *Bulletin of the American Meteorological Society*, 98(8), 1717–1737. https://doi.org/10.1175/BAMS-D-15-00308.1

Skamarock, W. C., Klemp, J. B., Dudhia, J., Gill, D. O., Liu, Z., Berner, J., Wang, W., Powers, J. G., Duda, M. G., Barker, D. M., & Huang, X.-Y. (2019). *A Description of the Advanced Research WRF Model Version 4* (NCAR Technical Notes NCAR/TN-556+STR). National Center for Atmospheric Research. https://doi.org/10.5065/1dfh-6p97

Thompson, G., Field, P. R., Rasmussen, R. M., & Hall, W. D. (2008). Explicit Forecasts of Winter Precipitation Using an Improved Bulk Microphysics Scheme. Part II: Implementation of a New Snow Parameterization. *Monthly Weather Review*, 136(12), 5095-5115. https://doi.org/10.1175/2008MWR2387.1

Turner, J., Lu, H., White, I., King, J. C., Phillips, T., Hosking, J. S., Bracegirdle, T. J., Marshall, G. J., Mulvaney, R., & Deb, P. (2016). Absence of 21st century warming on Antarctic Peninsula consistent with natural variability. *Nature*, 535, 411–415. https://doi.org/10.1038/nature18645

Zhang, C., & Zhang, J. (2018). Modeling Study of Foehn Wind Events in Antarctic Peninsula with WRF Forced by CCSM. *Journal of Meteorological Research*, 32, 909–922. https://doi.org/10.1007/s13351-018-8067-9

Received: 23 October 2020
Accepted: 24 December 2020

Д. Пішняк*, Б. Безнощенко

Державна установа Національний антарктичний науковий центр МОН України,
м. Київ, 01601, Україна

*** Автор для кореспонденції**: den.meteo.is@gmail.com

Покращення деталізації моделювання атмосферних процесів за допомогою моделі Polar WRF на прикладі випадку сильних опадів у районі антарктичної станції «Академік Вернадський»

Реферат. Регіон Антарктичного півострова становить підвищений інтерес у зв'язку з особливостями змін клімату та механізмами атмосферної циркуляції. Регіональна мезомасштабна модель атмосфери Polar Weather Research and Forecast (WRF) (Полярна модель дослідження і прогнозування погоди) v4.1.1 використана для дослідження випадку сильних опадів над районом Української антарктичної станції «Академік Вернадський» (Антарктичний півострів). Попередньо був обраний типовий синоптичний процес перевалювання циклону через Антарктичний півострів, який, в той же час, приніс найбільшу добову кількість опадів у 2018 році. Оцінка якості моделювання та виконання деталізації зроблені шляхом порівняння результатів з фактичними вимірами на станції «Академік Вернадський» та крос-доменним відстеженням значень осереднених метеорологічних величин і відхилень. Застосування технології вкладених розрахункових областей дозволили підвищити горизонтальну роздільну здатність змодельованої атмосфери до 1 км і, таким чином, детально відтворити вітровий режим регіону. Порівняння з фактичними вимірами показує суттєве покращення моделювання вітрового режиму зі збільшенням роздільної здатності, але деяке погіршення представлення приземної температури і вологості повітря. Polar WRF показала загальне охолодження температури

біля поверхні на 2 °С протягом періоду моделювання та збільшення кількості опадів на 4,6–8,4 мм (12–21%) в середньому по всій території відносно вихідних даних Global Data Assimilation System (Глобальна система асиміляції даних). Це може пояснюватися вкладом шумів та недосконалістю моделі (включаючи статичні вхідні дані опису місцевості). Як показав фізичний аналіз результатів моделювання, взаємодія вітрового потоку з гірським рельєфом Антарктичного півострова створює ряд складних динамічних ефектів в атмосфері, які в свою чергу формують локальні максимуми опадів як над хребтом півострова так і над прилеглою акваторією океану. Це, відповідно, затоко-долинні області підсилення опадів та підсилення опадів на гребенях ударних хвиль від орографічних перешкод. За певних фонових вітрових умов, вплив останнього ефекту може досягати станції «Академік Вернадський» і призводити до формування сильних опадів.

Ключові слова: Антарктичний півострів, мезомасштабні атмосферні процеси, пониження масштабу, статистичне оцінювання, ефекти підсилення опадів, численне моделювання атмосфери